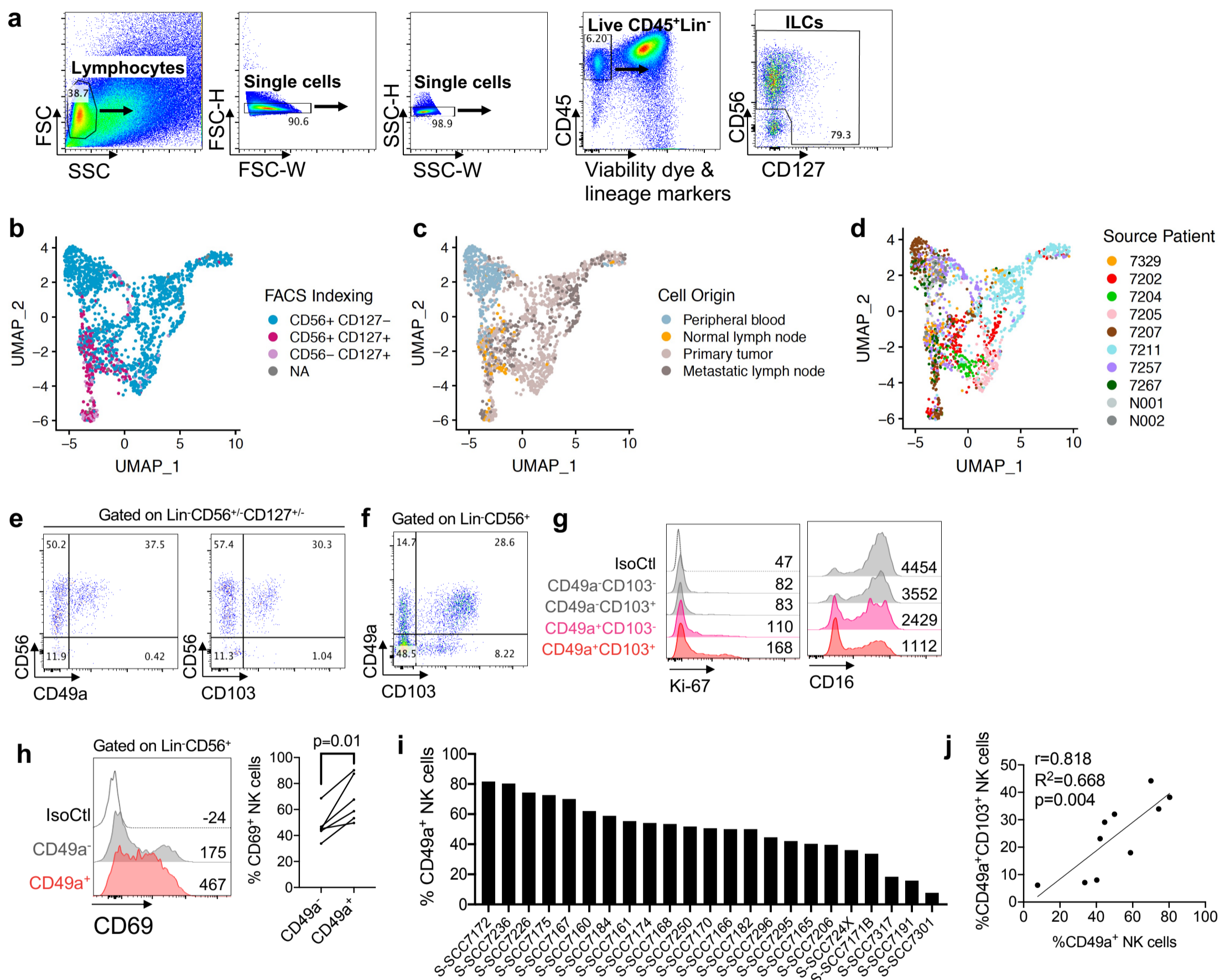


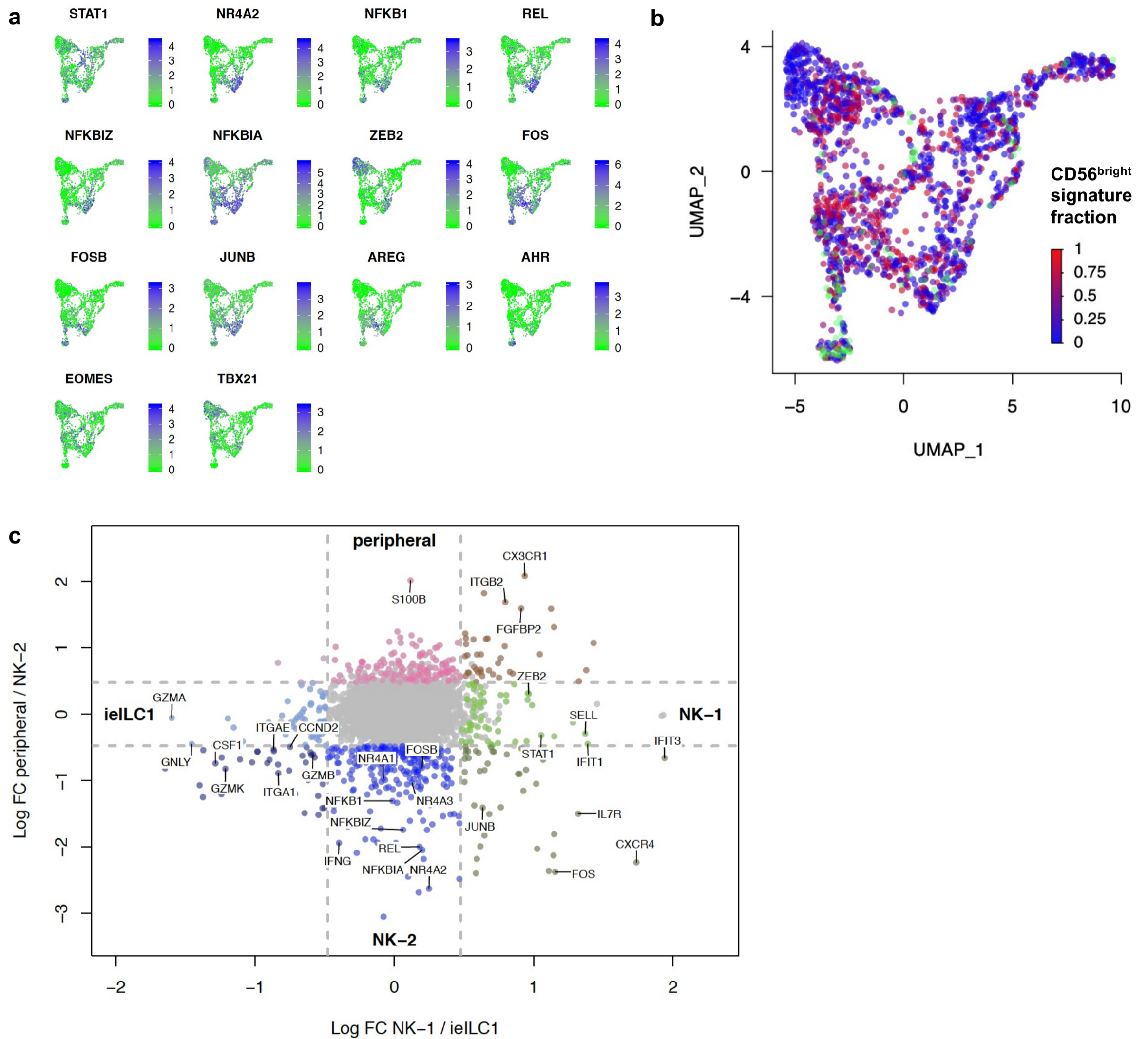
SUPPLEMENTAL INFORMATION

Supplemental Figure 1. Heterogeneity of ILCs in human HNSCC.



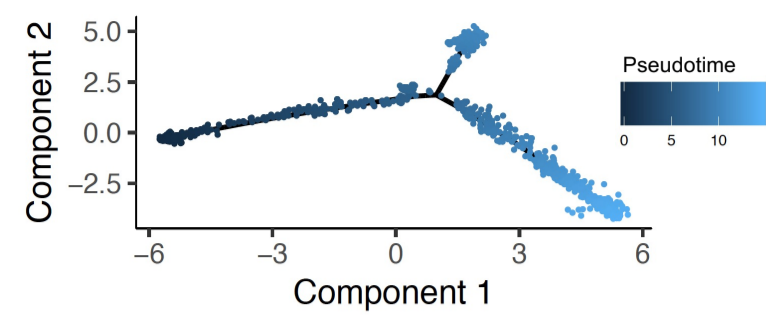
Supplemental Figure 1. Heterogeneity of ILCs in human HNSCC. (a) Gating strategy to sort intratumoral ILCs cell for scRNA-seq analysis. Live non-doublet CD45⁺Lineage⁻ (e.g. CD3⁻CD14⁻CD19⁻CD20⁻CD34⁻CD68⁻) lymphocyte gating was used to single-cell sort CD56^{+/-}CD127^{+/-} cells into 96-well plates for single-cell RNA-sequencing. This gating strategy included NK cells and the known subsets of ILCs. (b-d) UMAPs labelled by FACS indexin, cell origin, and patient source. UMAP plots labelled according to (b) CD56 and CD127 expression based on FACS indexing of sorted cells, (c) tissue of origin, and (d) patient sample source. (e-j) Phenotypic characterization of intratumoral NK cells based on CD49a expression. Single-cell suspensions of human HNSCC tumor samples were stained for surface and intracellular markers and analyzed by flow cytometry. (e) CD49a and CD103 expression on Lin⁻CD56^{+/-}CD127^{+/-} population (as described in (a)). (f) Expression of CD49a and CD103 on Lin⁻CD56⁺ cells. (g) Expression of Ki-67 and CD16 on gated CD49a⁻CD103⁻, CD49a⁻CD103⁺, CD49a⁺CD103⁻, and CD49a⁺CD103⁺ cells. Plots and histograms show representative examples of the phenotype observed on cells from at least four donors. (h) Expression of CD69 on Lin⁻CD56⁺CD49a⁻ or Lin⁻CD56⁺CD49a⁺ cells. (left) Histogram shows a representative example, and (right) graph shows cumulative results from six different donors; paired *t*-test analysis was done, and *p* value is shown. (i) Heterogeneity in the percentage of Lin⁻CD56⁺CD49a⁺ cells among HNSCC from different patients. (j) Correlation between the percentage of Lin⁻CD56⁺CD49a⁺ cells and the percentage of Lin⁻CD56⁺CD49a⁺CD103⁺ cells in HNSCC from different patients.

Supplemental Figure 2. Gene expression profiles across the ILC spectrum.



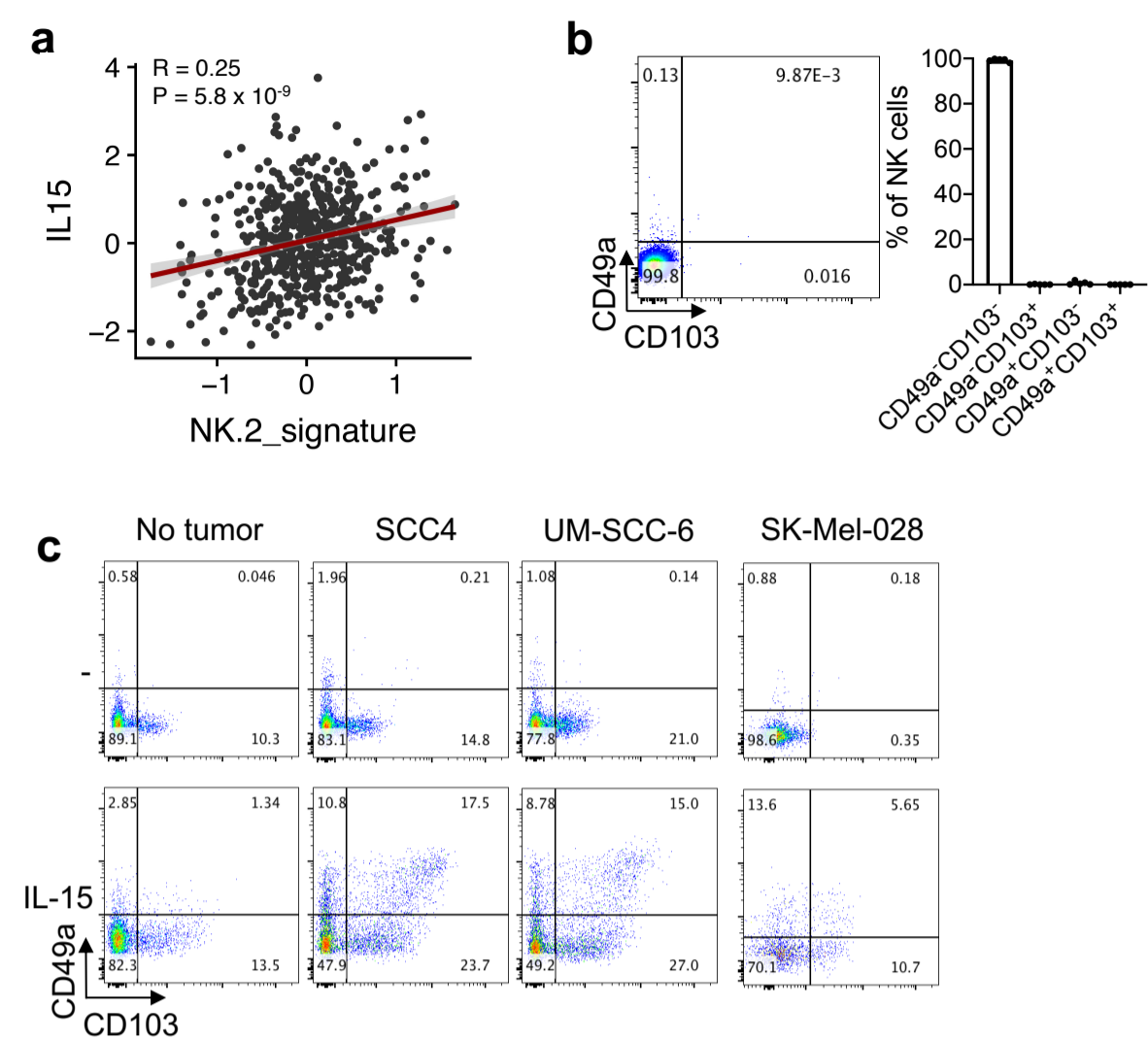
Supplemental Figure 2. Gene expression profiles across the ILC spectrum. (a) Feature plots showing the expression of transcription factors (STAT1, NFKB1, REL, ZEB2, FOS, FOSB, JUNB, AHR, EOMES, TBX21) and mediators of NF κ B signaling (NFKBIA, NFKBIZ), among the ILC clusters in UMAP shown in Fig. 1b. (b) CIBERSORTx deconvoluted CD56^{bright} signature fraction in human intra-tumoral and peripheral ILCs. CIBERSORTx fractions were determined for each single-cell gene expression library in this study, based on gene expression signatures derived from Collins et al. (2019)³⁵. For FACS-sorted CD56⁺ cells, the CD56^{bright} signature fraction was calculated by the following signature proportion: CD56^{bright} / (CD56^{bright} + CD56^{dim}). FACS-sorted CD56⁻ cells are represented in green on the plot. (c) Log fold-change plot showing gene expression differences among peripheral NK, NK-1, NK-2 and ielLC1 populations. Colored dots (as opposed to gray) represent transcripts expressed at least 3-fold higher in one subset versus another.

Supplemental Figure 3. Pseudotime trajectory analysis.



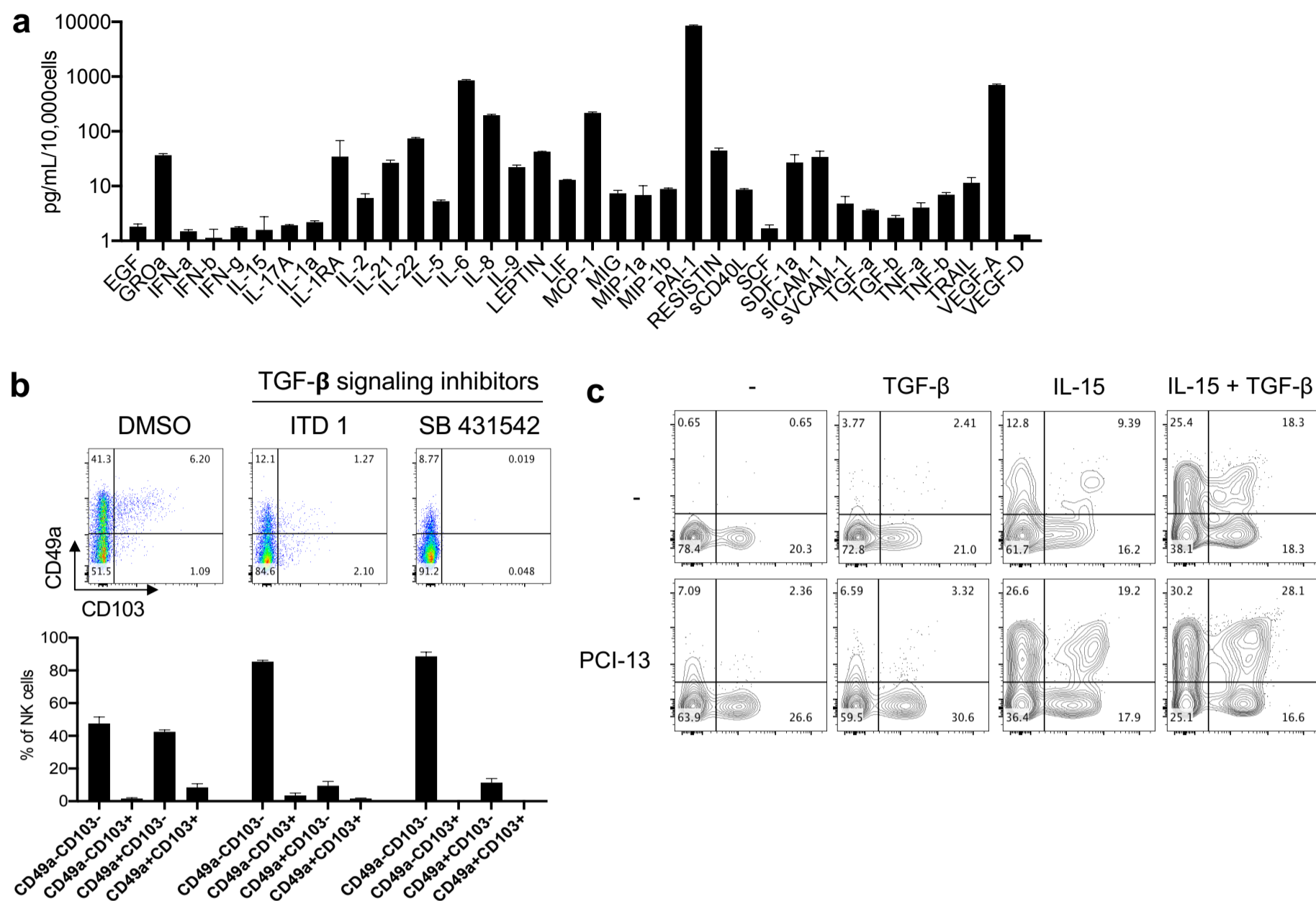
Supplemental Figure 3. Pseudotime trajectory analysis. Pseudotime trajectories of cells that had primarily NK cell signatures, determined by CIBERSORTx deconvolution of the subset clusters, demonstrated two possible differentiation trajectories from peripheral NK cells: an end-state of either the NK-2 phenotype or the ielLC1 phenotype.

Supplemental Figure 4. Peripheral NK cells differentiate into ielLC1-like cells, *in vitro*.



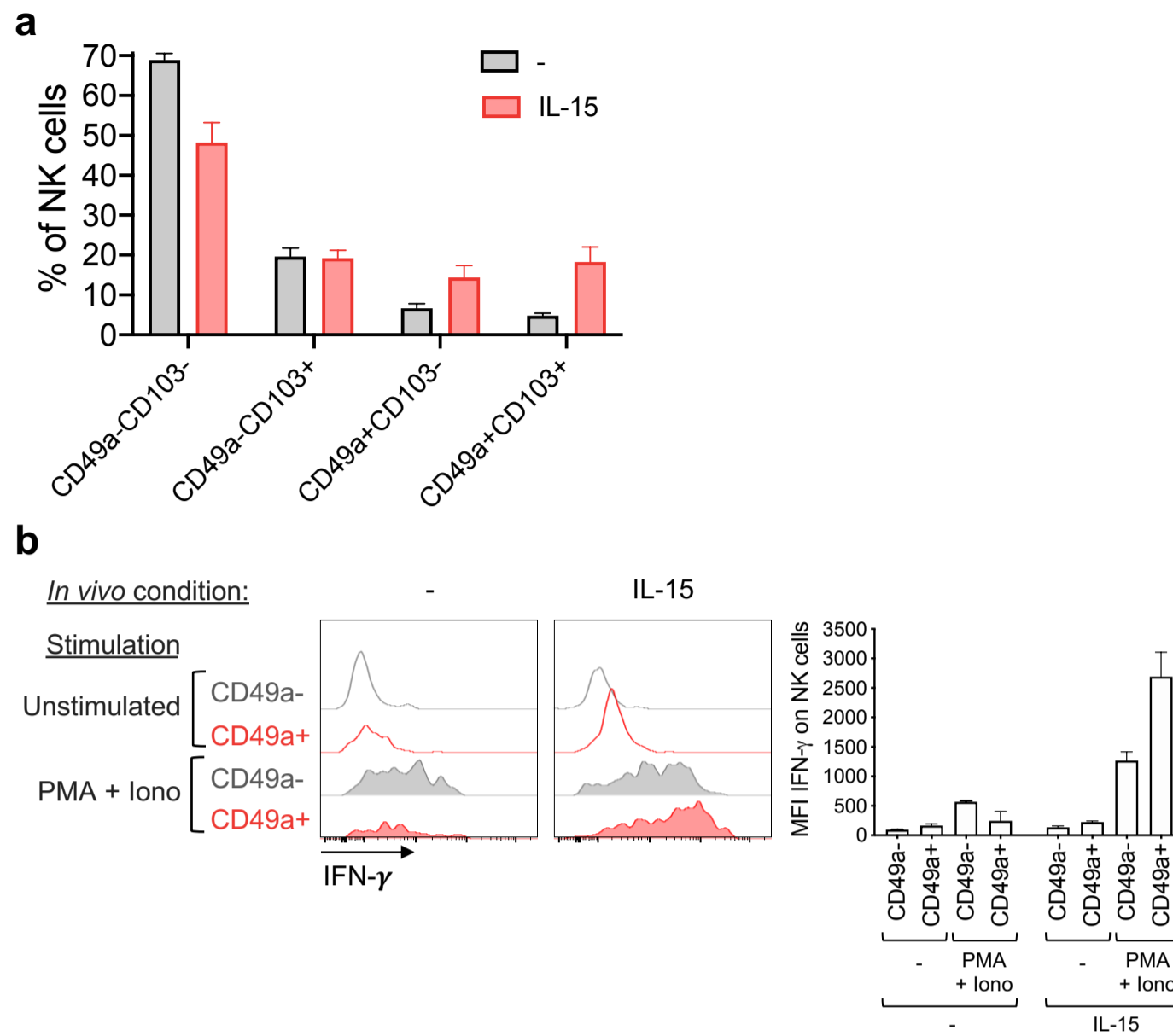
Supplemental Figure 4. Peripheral NK cells differentiate into ielLC1-like cells, *in vitro*. (a) Correlation between *IL15* gene expression in human HNSCC tumors from the TCGA database and an NK-2 gene expression signature obtained from the scRNA-seq data. (b) Expression of CD49a and CD103 on peripheral NK cells from healthy donors. (left) Dot plot shows a representative example, and (right) graph shows cumulative results from cells from 5 different donors. (c) Peripheral NK cells were co-cultured with SCC4 or UM-SCC-6 HNSCC cells, or SK-Mel-028 melanoma cells (at E:T = 10:1), in the presence or not of IL-15 (10ng/mL), as described in Fig. 4b. Dot plots show one representative example of the expression of CD49a and CD103 on NK cells after culture from two independent experiments, using NK cells from different donors.

Supplemental Figure 5. TGF- β and IL-15 induce the ielLC1-like phenotype.



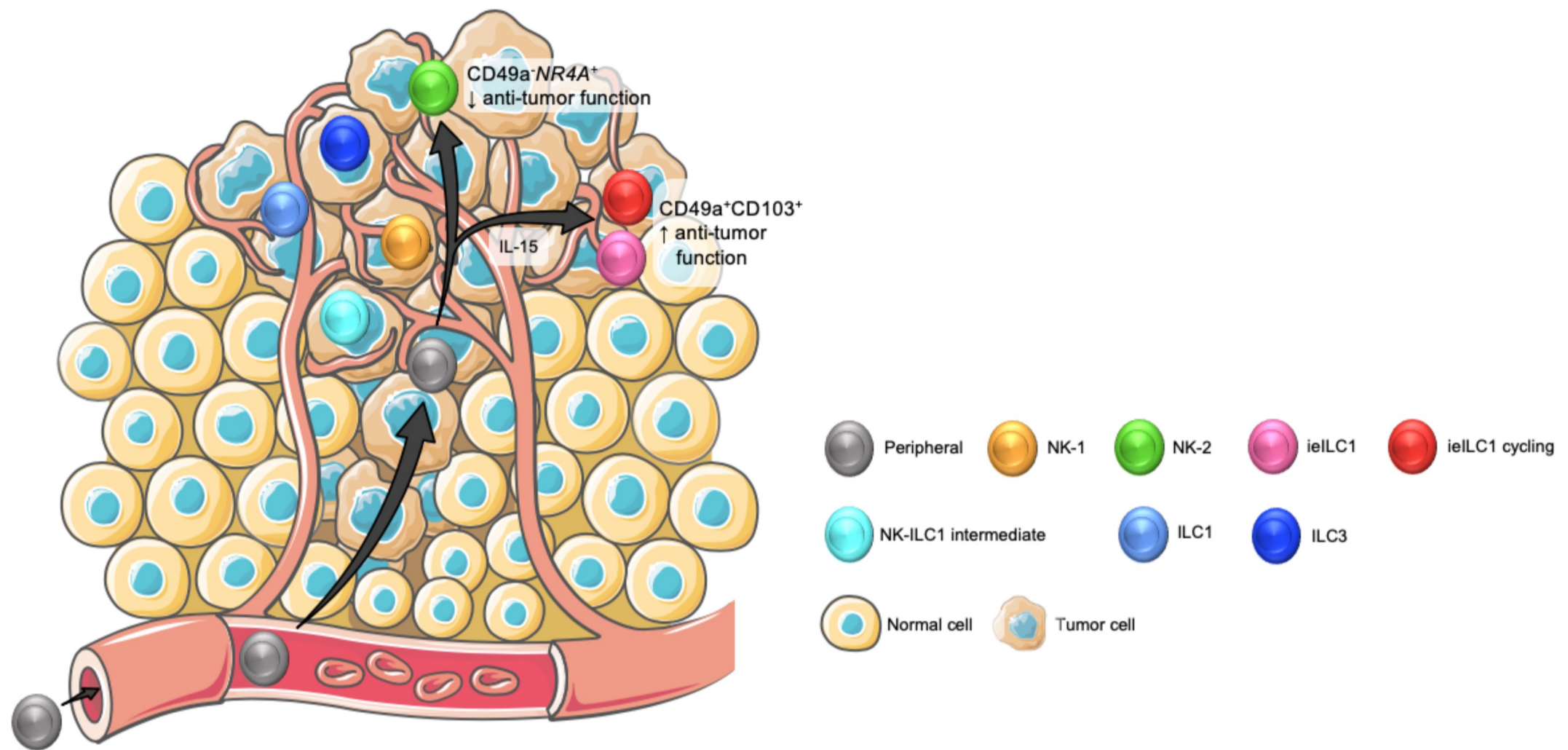
Supplemental Figure 5. TGF- β and IL-15 induce the ielLC1-like phenotype. (a) Cytokines and chemokines secreted by PCI-13 cells. PCI-13 cells were cultured for 3 days; then supernatants were harvested and a 62-plex Luminex Immuno-Assay was performed. Graph shows cytokines and chemokines secreted by PCI-13, in duplicate measurements. Graph is expressed as mean \pm SEM. (b) Peripheral NK cells were co-cultured with PCI-13 HNSCC cells (at E:T = 10:1) and IL-15 (10ng/mL), in the presence of TGF- β signaling inhibitors ITD 1 (10 μ M) or SB 431542 (10 μ M). (b, top) Dot plots show one example of the expression of CD49a and CD103 on NK cells after 4 days of culture. (b, bottom) Graph shows cumulative results from three independent experiments, using NK cells from different donors. Graph is expressed as mean \pm SEM. (c) Peripheral NK cells were cultured with or without PCI-13 HNSCC cells (at E:T = 10:1) in the presence of TGF- β , IL-15 or IL-15 + TGF- β (10ng/mL each), similar to Fig. 4b. Dot plots show one example of the expression of CD49a and CD103 on NK cells after culture from three independent experiments, using NK cells from different donors.

Supplemental Figure 6. Functional analysis of *in vivo*-differentiated ielLC1-like cells.



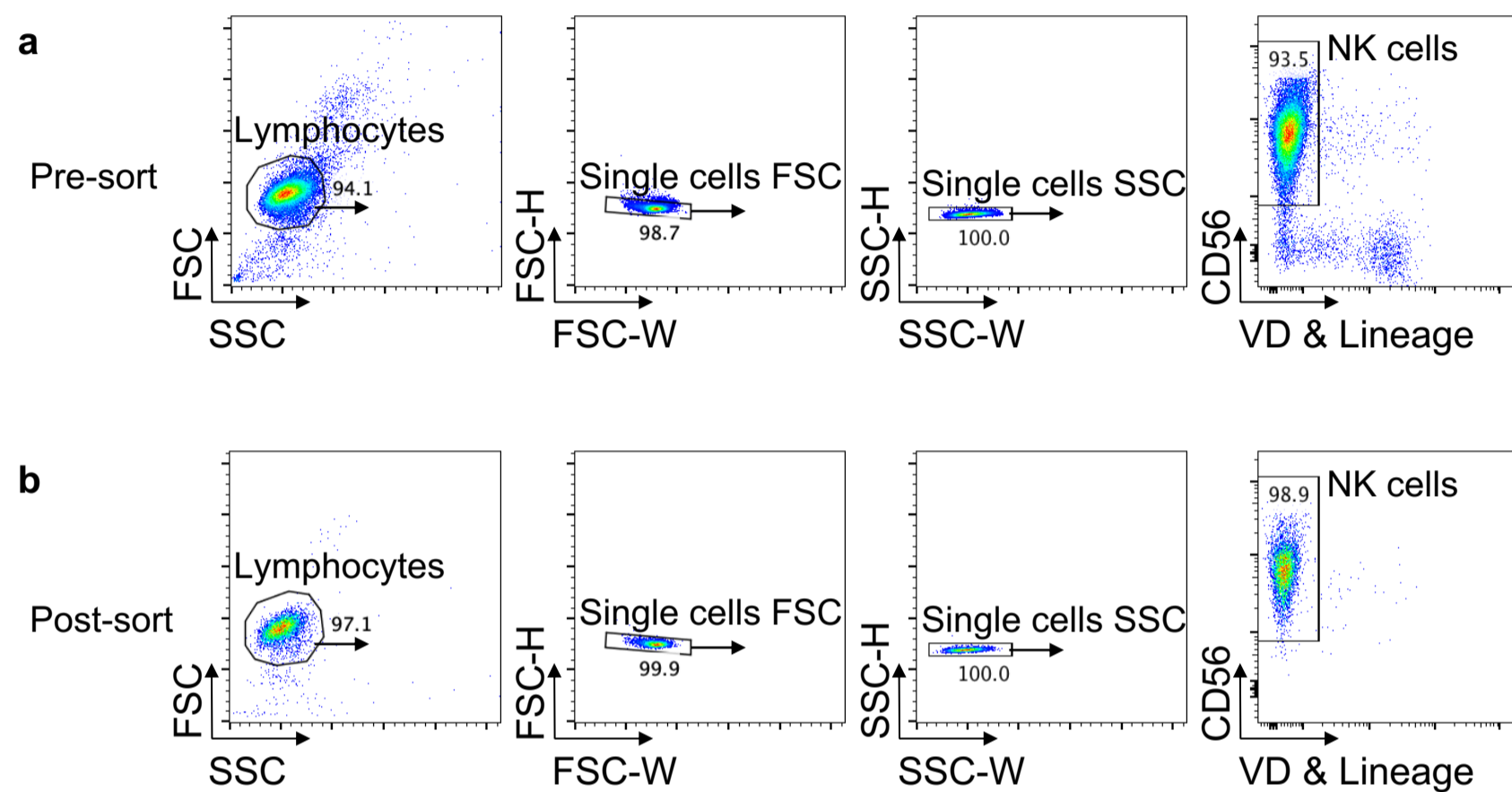
Supplemental Figure 6. Functional analysis of *in vivo*-differentiated ielLC1-like cells. (a) Sorted peripheral bulk NK cells were differentiated *in vivo* into ielLC1-like cells using the protocol described in Fig. 7a. After *in vivo*-differentiation, the phenotype of intratumoral NK cells was determined. Graphs show cumulative results from one representative experiment, using NK cells from one donor. (b) Sorted peripheral CD56^{bright} NK cells were differentiated *in vivo* into ielLC1-like cells using the protocol described in Fig. 7a. After *in vivo*-differentiation, the ability of the cells to produce IFN γ in response to PMA and ionomycin stimulation was evaluated. (left) Histograms show a representative example of IFN γ production by CD45⁺Lin⁻CD56⁺CD49a⁻ and CD45⁺Lin⁻CD56⁺CD49a⁺. (right) Graphs show cumulative results from one representative experiment, using NK cells from one donor. Graphs were expressed as mean \pm SEM.

Supplemental Figure 7. Graphical illustration of intratumoral NK cell states.



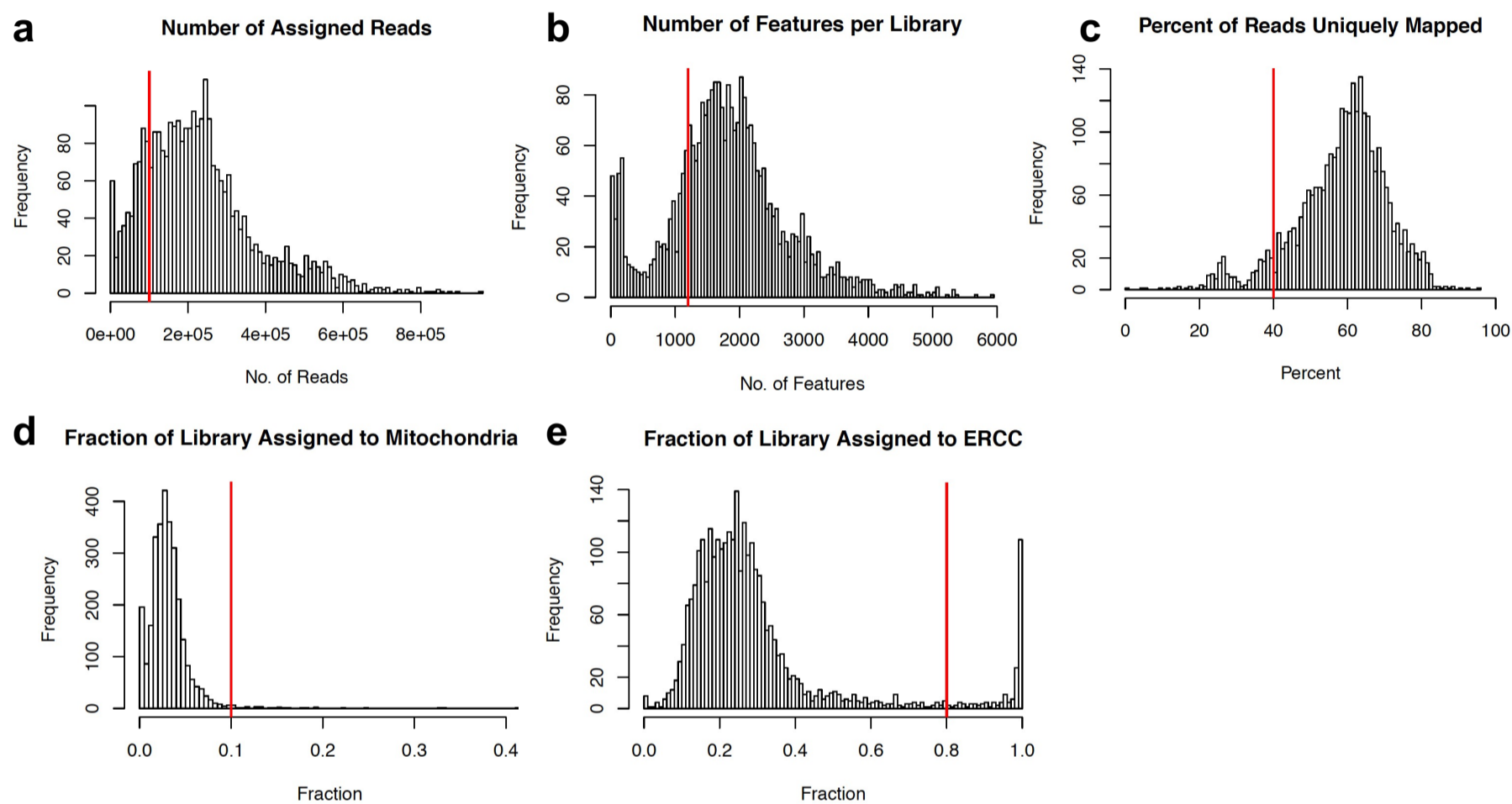
Supplemental Figure 7. Graphical illustration of intratumoral NK cell states. Model of intratumoral NK cell states. Eight different subsets of ILCs were observed within the tumor microenvironment of human HNSCC. Together, *in silico*, *in vitro*, and *in vivo* studies indicate that peripheral conventional NK cells differentiate along different trajectories within the tumor to give rise to two functionally and phenotypically different end-states: NK-2 and ielLC1-like cells. The ielLC1-like cells are characterized by potent anti-tumor function; whereas, the NK-2 cells have poor anti-tumor function. Cartoon image adaptations credit: Servier Medical Art, licensed under CC BY 3.0

Supplemental Figure 8. FACS sorting of peripheral NK cells.



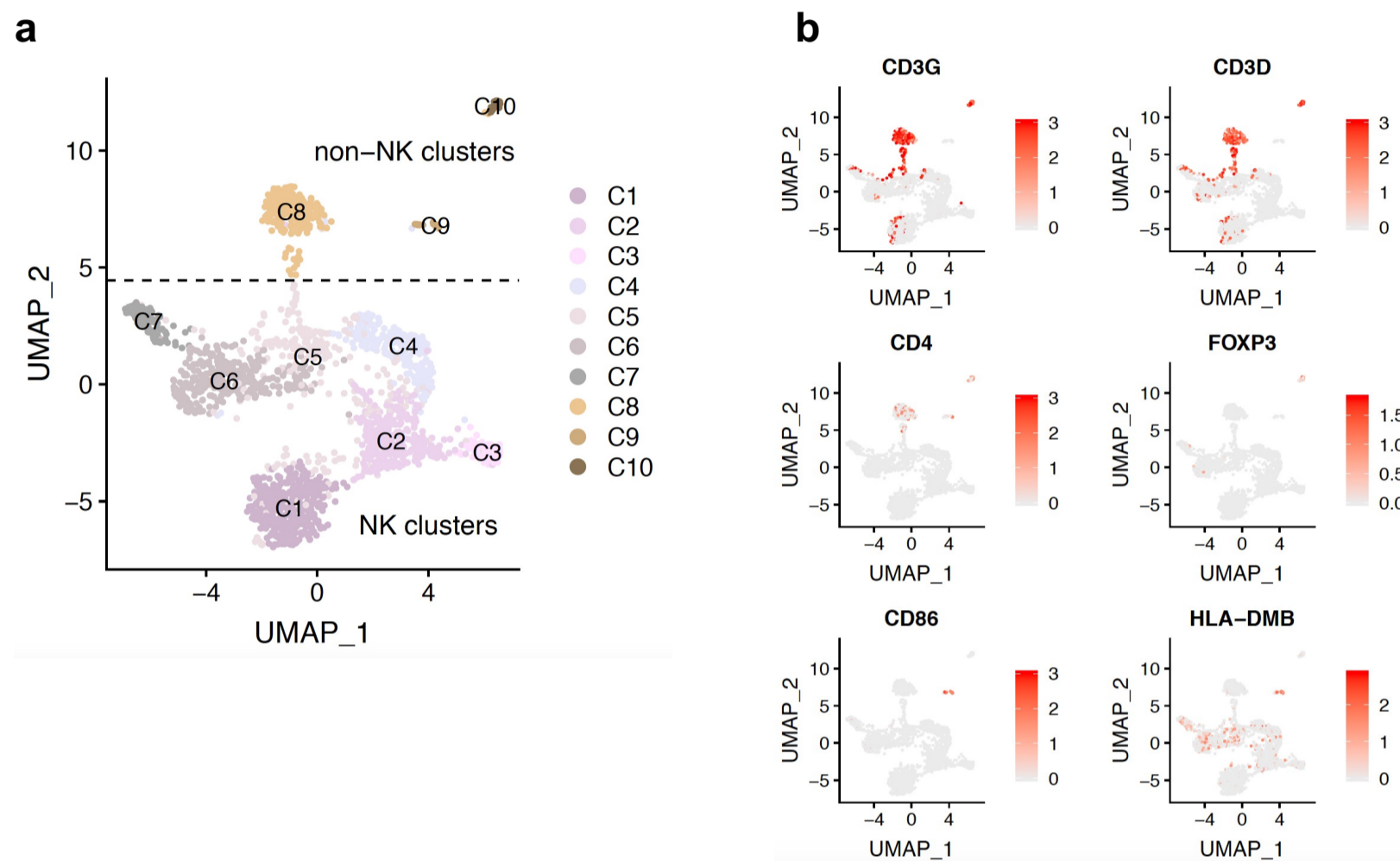
Supplemental Figure 8. FACS sorting of peripheral NK cells. (a-b) Dot plots show the gating used to purity sort NK cells from peripheral blood of healthy volunteers. Cells were gated as non-doublet lymphocytes live (VD⁻) Lineage⁻ (i.e. CD3⁻CD5⁻CD14⁻CD19⁻CD20⁻) CD56⁺. A representative example of (a) pre-sort and (b) post-sort plots is shown, from at least 10 sorts from different donors.

Supplemental Figure 9. Quality control metrics and cut-offs used for scRNA-seq data analysis.



Supplemental Figure 9. Quality control metrics and cut-offs used for scRNA-seq data analysis. Distribution of sequenced libraries based on (a) number of reads successfully assigned to GENCODE gene transcripts, (b) number of gene features represented in each library, (c) percentage of reads uniquely mapped by STAR-aligner, (d) fraction of mitochondrial reads in each library and (e) fraction of reads in each library assigned to ERCC92 transcripts. Selection criteria for high-quality libraries indicated in red, based on (1) library size > 100,000 counts, (2) represented features > 1200, (3) uniquely mapped reads > 40%, (4) mitochondrial fraction < 10%, (5) ERCC mapped reads < 80%.

Supplemental Figure 10. Initial clustering of single cells, before filtering for non-NK clusters.



Supplementary Figure 10. Initial clustering of single cells, before filtering for non-NK clusters. (a) UMAP before filtering for non-NK clusters. **(b)** Gene expression of selected markers for clusters C8, C9 and C10.

Supplemental Table 1. List of antibodies used.

Specificity	Fluorophore	Clone	Catalog #	Vendor
CD3	APC-Cy7	UCHT1	300426	BioLegend
CD5	APC-Cy7	L17F12	364010	BioLegend
CD14	APC-Cy7	HCD14	325620	BioLegend
CD16	Pacific Blue	3G8	302021	BioLegend
CD19	APC-Cy7	HIB19	302218	BioLegend
CD20	APC-Cy7	2H7	302314	BioLegend
CD34	APC-Cy7	561	343614	BioLegend
CD45	BV605	2D1	368524	BioLegend
CD49a	BUV395	SR84	742363	BD Biosciences
CD49a	FITC	TS2/7	328307	BioLegend
CD49a	PE	TS2/7	328303	BioLegend
CD56	BUV737	NCAM16.2	564447	BD Biosciences
CD56	PE-Cy5	B159	555517	BD Biosciences
CD69	APC	FN50	310909	BioLegend
CD94	APC	DX22	305508	BioLegend
CD94	FITC	DX22	305504	BioLegend
CD103	FITC	Ber-ACT8	350203	BioLegend
CD103	PE-Cy7	Ber-ACT8	350211	BioLegend
CD107a	FITC	H4A3	555800	BD Biosciences
CD117	APC	104D2	313205	BioLegend
CD117	BV785	104D2	313237	BioLegend
CD117	PE-Cy7	104D2	313211	BioLegend
CD127	PE	A019D5	351303	BioLegend
CD127	PE-Cy5	A019D5	351324	BioLegend
CRTH2 (CD294)	PE/Dazzle 594	BM16	350125	BioLegend
Eomes	Alexa Fluor 700	644730	IC6166N	R&D Systems
Eomes	FITC	WD1928	11-4877-41	eBioscience
IFN- γ	PE-Cy7	4S.B3	557844	BD Biosciences
Ki67	APC	Ki-67	350513	BioLegend
Granzyme B	PE	GB12	MHGB04	Invitrogen
Granzyme B	PE/Dazzle 594	QA16A02	372215	BioLegend
NKp44	APC	P44-8	325110	BioLegend
NKp44	PE	P44-8	325107	BioLegend
NKp80	APC	REA845	130-112-591	Miltenyi Biotec
NKp80	PE	REA845	130-112-779	Miltenyi Biotec
PD-1	FITC	MIH4	11-9969-41	Invitrogen
PD-1	FITC	NAT105	367411	BioLegend
RORgt	PE	AFKJS-9	12-6988-80	eBioscience
T-bet	Alexa Fluor 647	4B10	644803	BioLegend
T-bet	PE-Cy7	eBio4B10 (4B10)	25-5825-80	eBioscience
TRAIL (CD253)	APC	RIK-2	308209	BioLegend